Revision to the Initial Assessment of the South African sardine resource using data from 1984-2018

C.L. de Moor*

Correspondence email: *carryn.demoor@uct.ac.za*

Introduction

This document presents a revision to the two mixing component assessment of South African sardine by de Moor (2019). This assessment remains an "initial assessment" with results expected to be sufficiently accurate such that they can reliably form the basis of simple constant catch projections for short-term management decisions. This is not the planned comprehensive assessment as detailed in the future work section of de Moor (2019).

Methods

There are only two differences between this revised model and the one by de Moor (2019). In all other aspects the model remains identical to that detailed in the Appendix of de Moor (2019). The data are also unchanged from that used by de Moor (2019).

The first difference is for a correction to the way growth is modelled. "Growth" in this model is taken to describe the increase in the expected length of a fish given an increase in its age. In de Moor (2019) the expected length of fish of age $a > 0$ in year y was assumed to be dependent on the timing of the recruits in year y. This revised model corrects this assumption such that the expected length of fish of age $a > 0$ in year y are assumed to be dependent on the timing of recruitment of *those same* fish. In other words, if recruits of a particular cohort arrive early (late) the length of fish of that cohort at age 1 and 2 etc. in this revised model are expected to be larger (smaller) than if the cohort recruited "on time". The expected growth (length) of individual fish over time is therefore modelled according to the von Bertalanffy growth curve (Figure 1). In contrast, the model of de Moor (2019) effectively allows the growth of fish of, for example, age 1 in year y, to speed up or slow down dependent on whether the recruits in year y are early or late. This can have some extreme cases where the expected length of fish decreases as they increase in age (Figure 1).

The changes to the equations of Appendix A of de Moor (2019) are in the growth curve used to generate the length at age matrix (equations (A7) and (A17)):

$$A^{sur}_{j,y,a,l} \sim N\left(L_{j,\infty}\left(1-e^{-\kappa_j(a-t_{0,j,y-a})}\right), \vartheta_a^2\right) \qquad y_1 \le y \le y_n, 0 \le a \le 5^+, 2.5^- cm \le l \le 24^+ cm$$

$$A^{com}_{j,y,q,a,l} \sim N\left(L_{j,\infty}\left(1-e^{-\kappa_j(a+(2q-1)/8-t_{0,j,y-a})}\right), \left[(1-(2q-1))\vartheta_a + (2q-1)\vartheta_{a+1}\right]^2\right)$$
$$y_1 \le y \le y_n, 1 \le q \le 4, 0 \le a \le 5^+, 2.5^- cm \le l \le 24^+ cm$$

where

$$t_{0,j,y} = \begin{cases} t_{0,j} + \varepsilon_y^t & y = y_1 \\ t_{0,j} + \rho^t \varepsilon_{y-1}^t + \sqrt{1-(\rho^t)^2}\varepsilon_y^t & y_1 < y \le y_n \end{cases}$$

and

$A^{sur}_{j,y,a,l}$ denotes the proportion of age a of component j sardine that falls in the length group l in November of year y,

* MARAM (Marine Resource Assessment and Management Group), Department of Mathematics and Applied Mathematics, University of Cape Town, Rondebosch, 7701, South Africa.

$A^{com}_{j,y,q,a,l}$ denotes the proportion of age a of component j sardine that falls in the length group l mid-way through quarter q of year y,

$L_{j,\infty}$ denotes the maximum length (in expectation) of component j,

κ_j denotes the somatic growth rate parameter for component j,

$t_{0,j,y}$ denotes the age at which the length (in expectation) is zero in year y,

$t_{0,j}$ denotes the average age at which the length (in expectation) is zero,

ϑ_a denotes the standard deviation of the distribution about the mean length for age a, and

ε^t_y denotes the annual residuals about the age at which the length is zero,

ρ^t denotes the autocorrelation coefficient in these residuals

The second difference between the models is that survey selectivity is now allowed to differ between components (coasts). This was a change previously identified by the sardine Task Team (de Moor 2019), and simple to implement, hence implemented now instead of delaying for the comprehensive assessment. Equation (A27) of Appendix A of de Moor (2019) now includes a j (component) subscript:

$$S^{survey}_{j,l} = \begin{cases} 0 & l = 2.5^{-}cm \\ \left[1 + exp\{-\left(l + 0.25 - S_{50,j}\right)/\delta_j\}\right]^{-1} & 3cm \leq l \leq 24^{+}cm \end{cases} \qquad y_1 \leq y \leq y_n$$

where

$S^{survey}_{j,l}$ denotes survey selectivity-at-length l in the November survey for component j,

$S_{50,j}$ denotes the length at which survey selectivity is 50% for component j, and

δ_j denotes the inverse of slope of survey selectivity-at-length ogive when selectivity is 50% for component j.

Results and Discussion

The contributions to the log likelihood from this model are compared in Table 1 to that of de Moor (2019) and that resulting when only the growth model is changed (i.e. survey selectivity is not component-specific).

Figures 2 to 13 show the model fit to data and associated estimated relationships. Figure 14 shows the model estimated November west component recruitment plotted against the effective west component spawning biomass (allowing for 8% of the south component spawning biomass to contribute to west coast effective spawning biomass). Figure 15 shows the model estimated exploitation rates, with the exploitation rate on the west component having increased in 2018 to 0.31, though lower than the 0.60 estimated in 2016.

Summary

This document has provided a revision to the initial 'ball-park' update to the sardine assessment. The model predicted November survey biomass in 2018 was 41 000t on the west coast, compared to the observation of 35 000t, and 280 000t on the south coast, compared to the observation on 56 000t. It estimates the sardine biomass in November 2018 to have been about 439 000t, with the west component consisting of only 57 000t. The west component effective spawning biomass is estimated at about 21 000t in November 2018, with the south component effective spawning biomass at around 128 000t. Figure 16 shows the numbers-at-age estimated in 2018 for this revised model compared to that of de Moor (2018).

References

de Moor CL. 2019. Assessment of the South African sardine resource using data from 1984-2018: Initial results at the joint posterior mode for the two mixing-component hypothesis. DAFF: Branch Fisheries Document FISHERIES/2019/FEB/SWG-PEL/01.

Table 1. The contributions to the objective function at the posterior mode for three alternative models. The ratio of the multiplicative bias in the recruit survey to that in the November survey, k_r^S/k_N^S, is given for diagnostic purposes.

		-ln(Likelihood)					-ln(Prior)					
Model	-ln(Post-erior)	Nov	Rec	Com Prop-at-length	Survey Prop-at-length	Preva-lence	k_{ac}^S	$move_{1,y}$	ε_y^t	k_N^S	k_r^S	k_r^S/k_N^S
de Moor (2019)	946.3	58.3	37.6	-426.2	-392.4	1655.9	-1.43	-30.5	44.9	0.73	0.47	0.65
Only Growth changed	935.2	58.3	39.6	-430.5	-379.8	1634.5	-1.41	-30.6	45.1	0.75	0.57	0.75
This model	923.8	56.6	38.4	-429.6	-383.6	1628.1	-1.44	-30.7	45.9	0.73	0.60	0.81

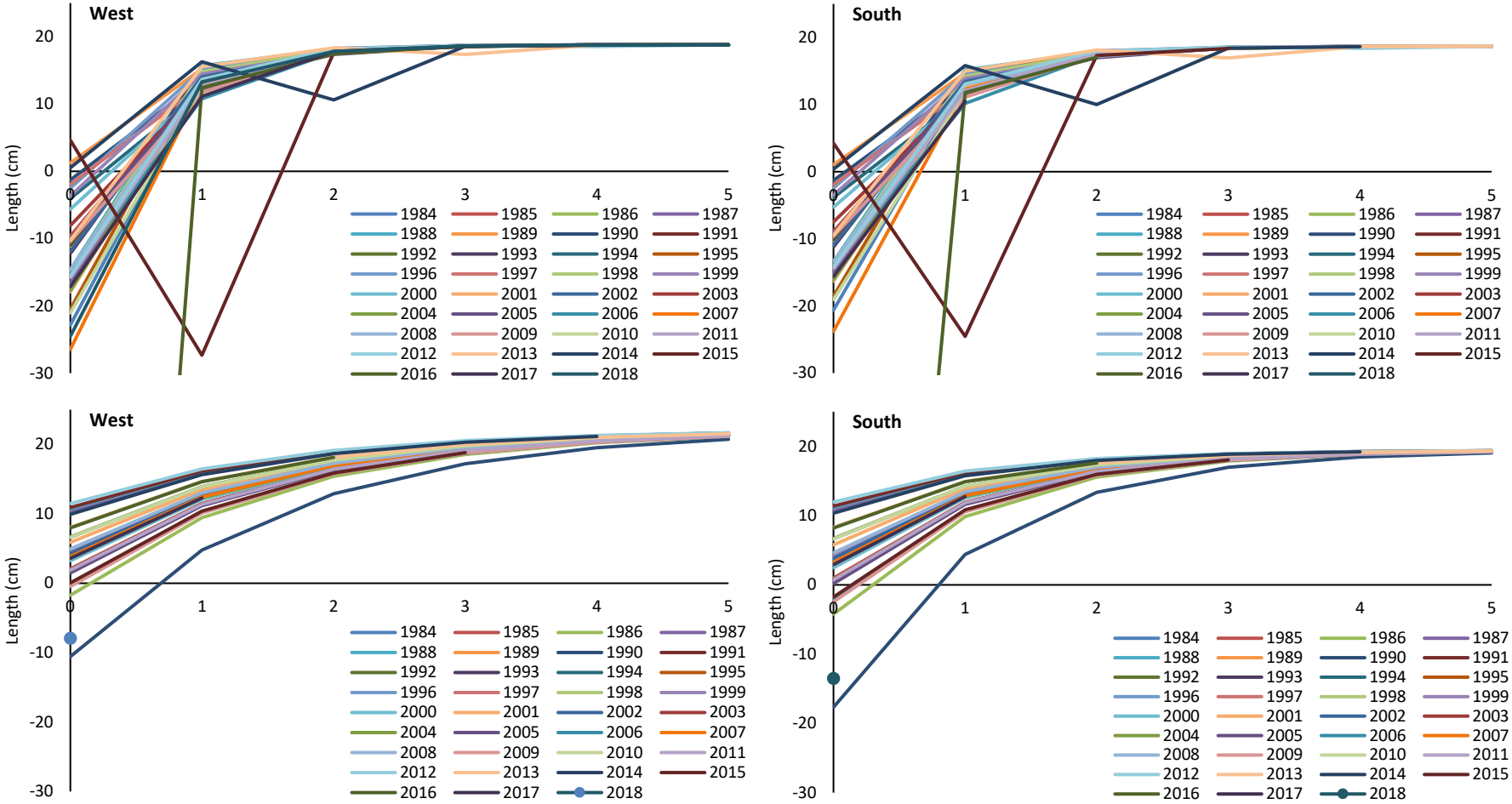

Figure 1. The expected growth of sardine according to de Moor (2019) (upper plots) and this revised model (lower plots). Each line corresponds to a different cohort of fish corresponding to recruitment in the labelled year.

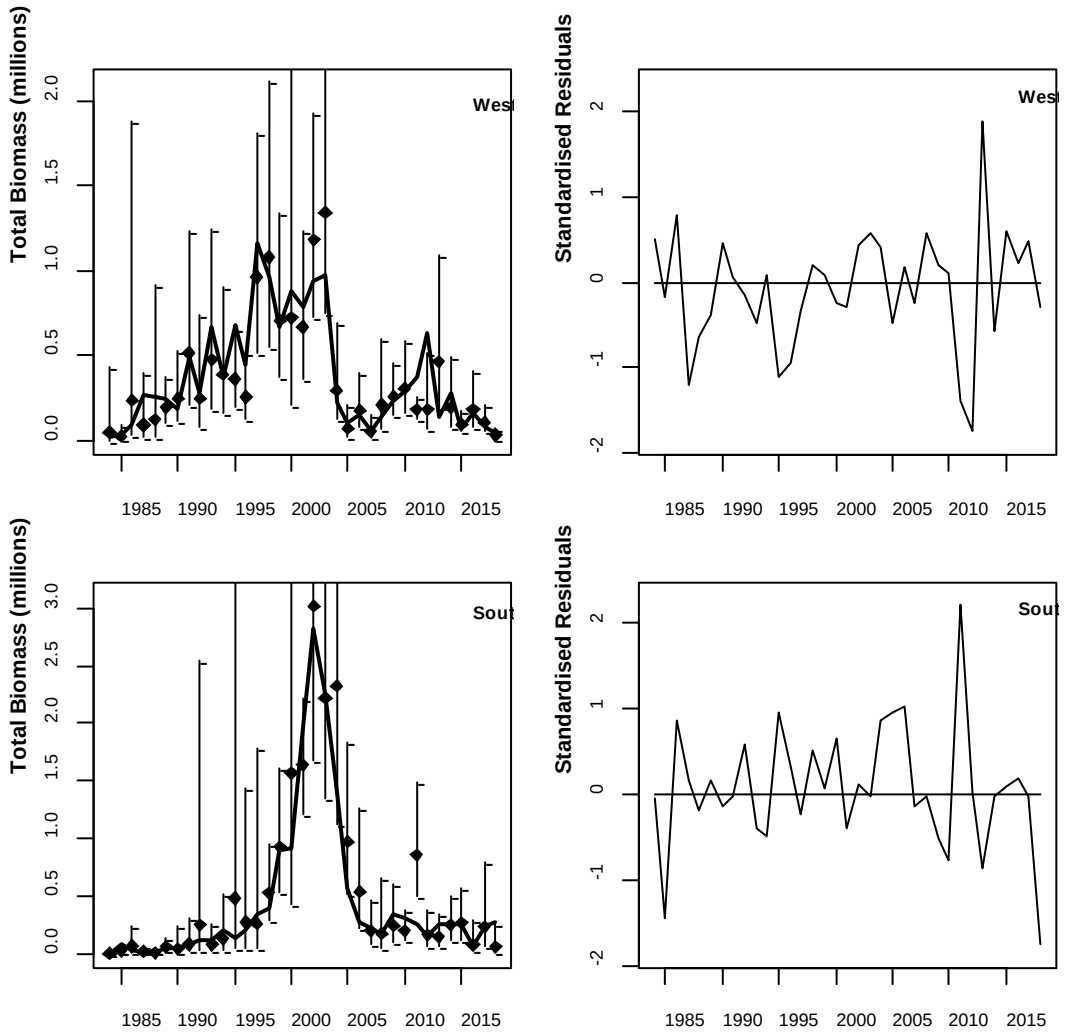

Figure 2. Acoustic survey estimated and model predicted November sardine total biomass from 1984 to 2018. The observed indices are shown with 95% confidence intervals. The standardised residuals (i.e. the residual divided by the corresponding standard deviation, including additional variance where appropriate) from the fits are given in the right hand plots.

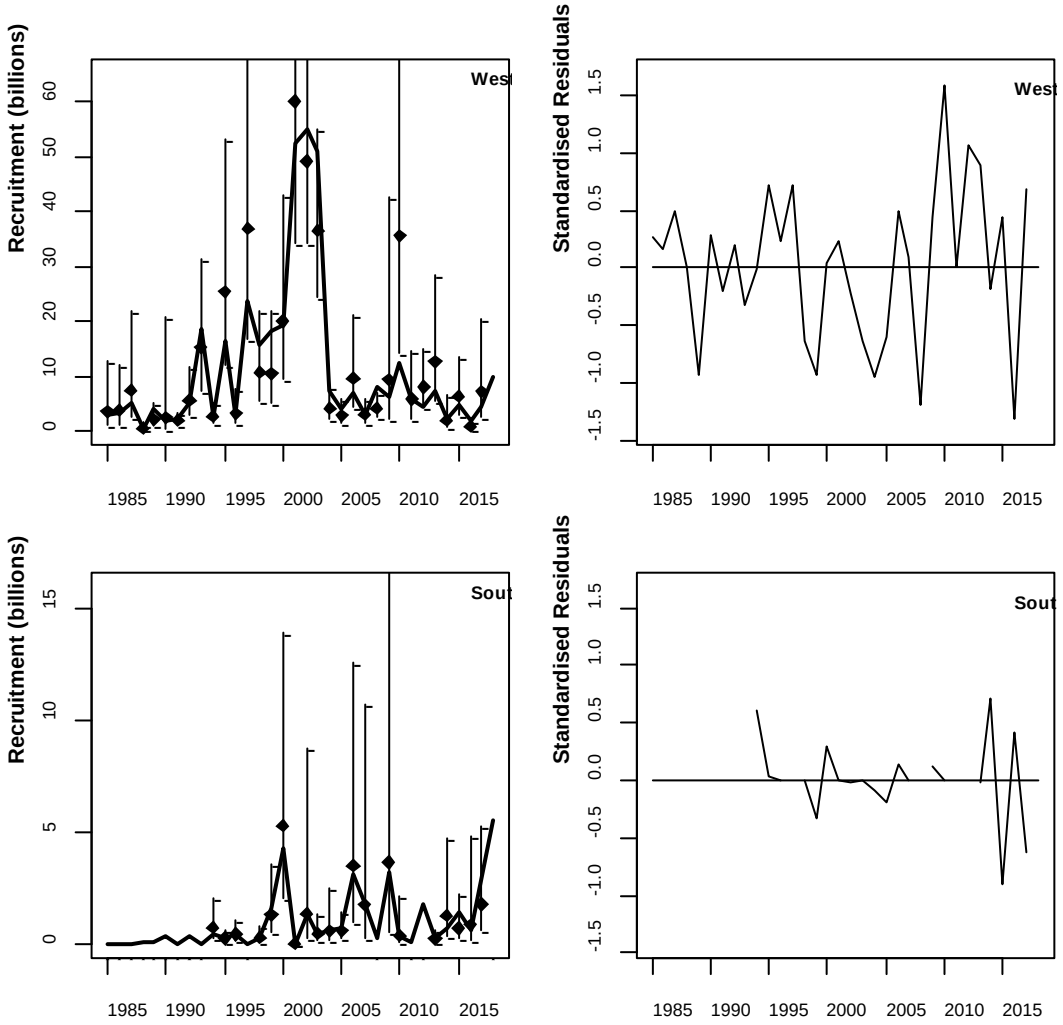

Figure 3. Acoustic survey estimated and model predicted sardine recruitment numbers from May 1985 to May 2018. The survey indices are shown with 95% confidence intervals. The standardised residuals from the fit are given in the right hand plots.

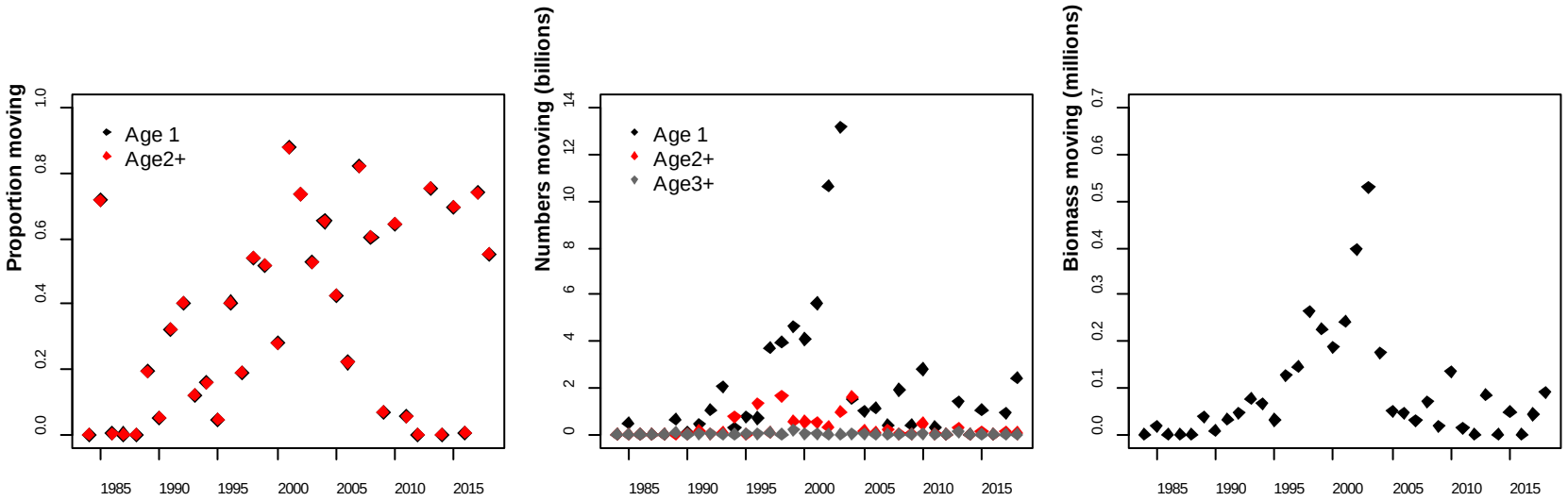

Figure 4. Model estimated proportion of 1-year-olds and 2+-year-olds which move from the "west" component to the "south" component in November. The middle plot shows the numbers of 1-, 2- and 3-year olds moving while the right hand plot shows rough estimates of the annual biomass moving from the west to south component.

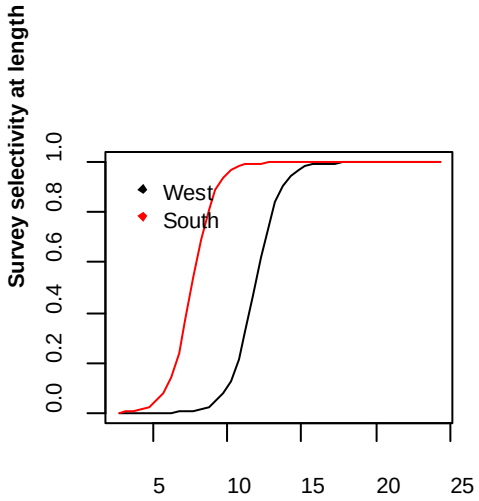

Figure 5. The model estimated November survey selectivity at length.

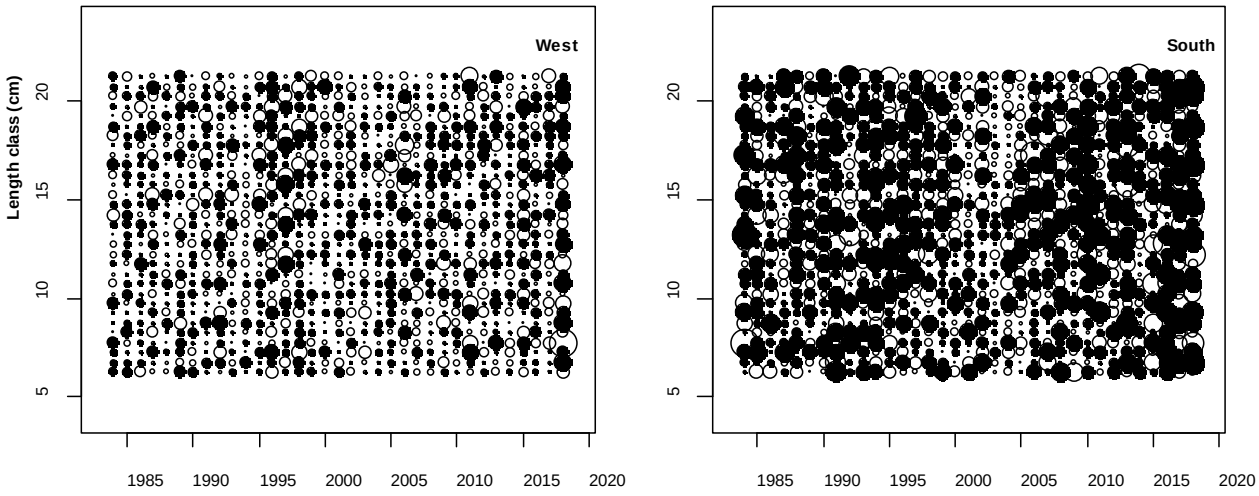

Figure 6. Residuals from the fit of the model predicted proportions-at-length in the November survey to the hydroacoustic survey estimated proportions.

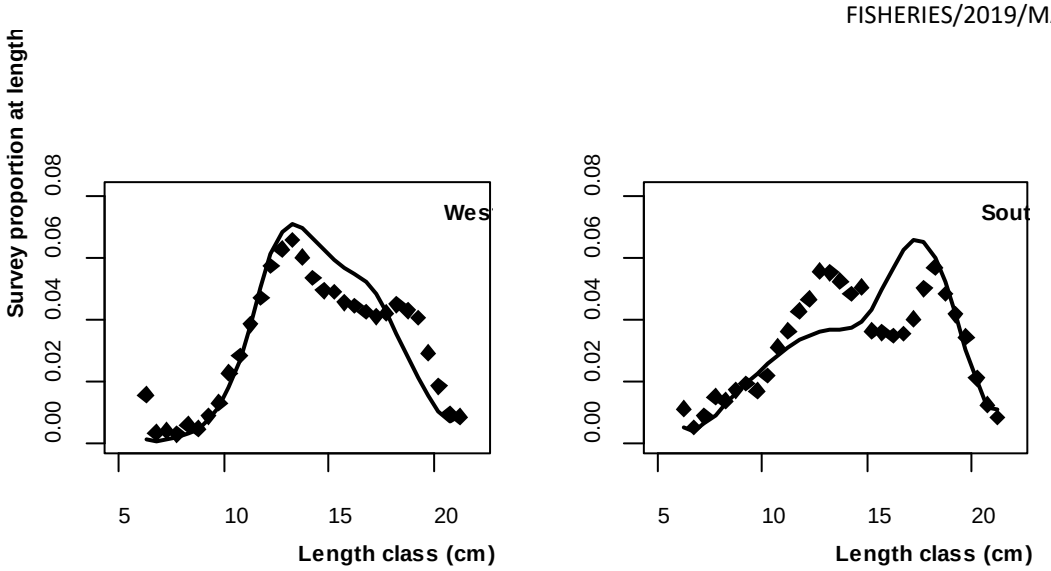

Figure 7. Average (over all years) model predicted and observed proportion-at-length in the November survey.

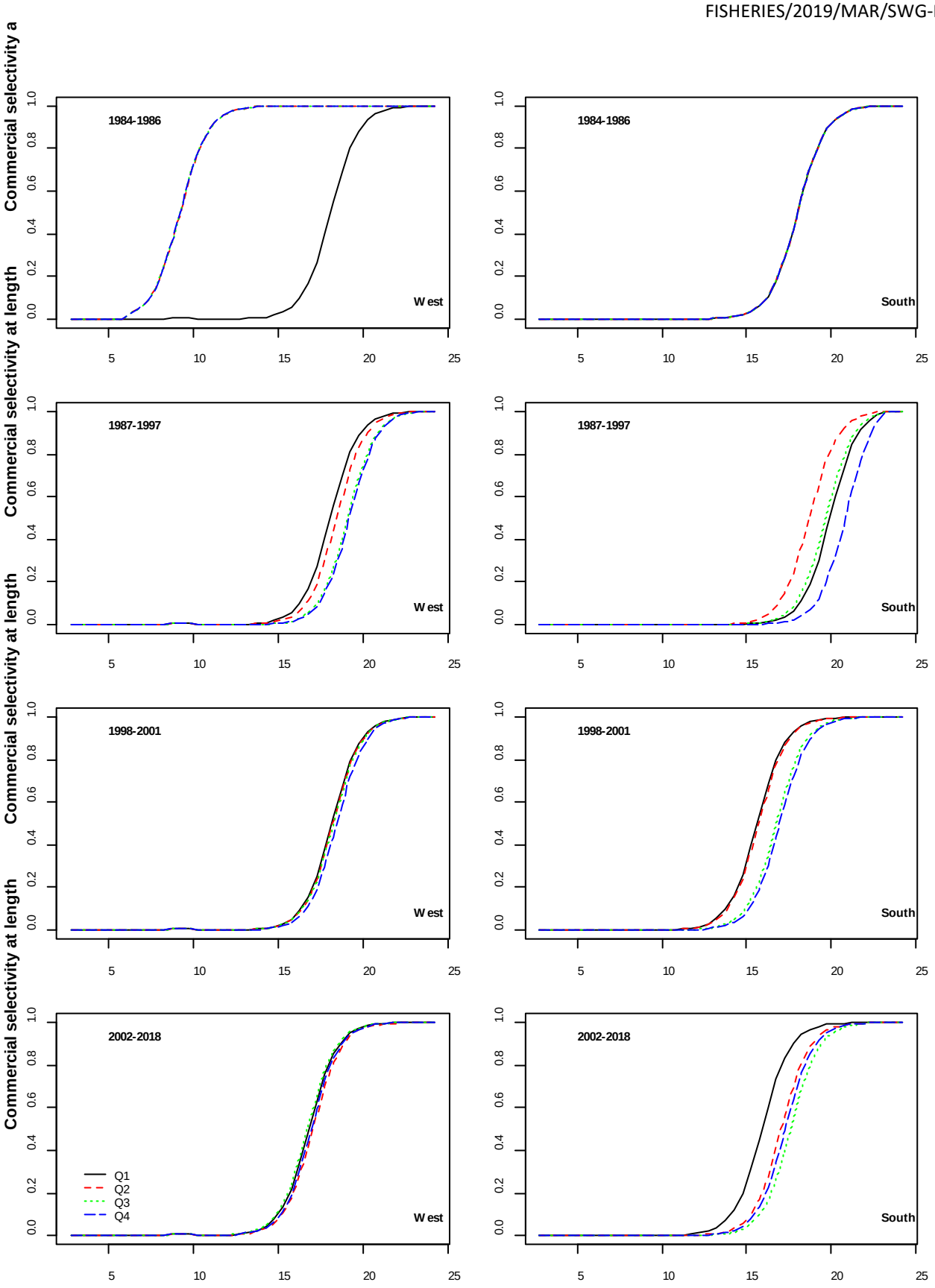

Figure 8. The model estimated commercial selectivity at length, which differs between four pre-specified time periods (the four rows) and quarters.

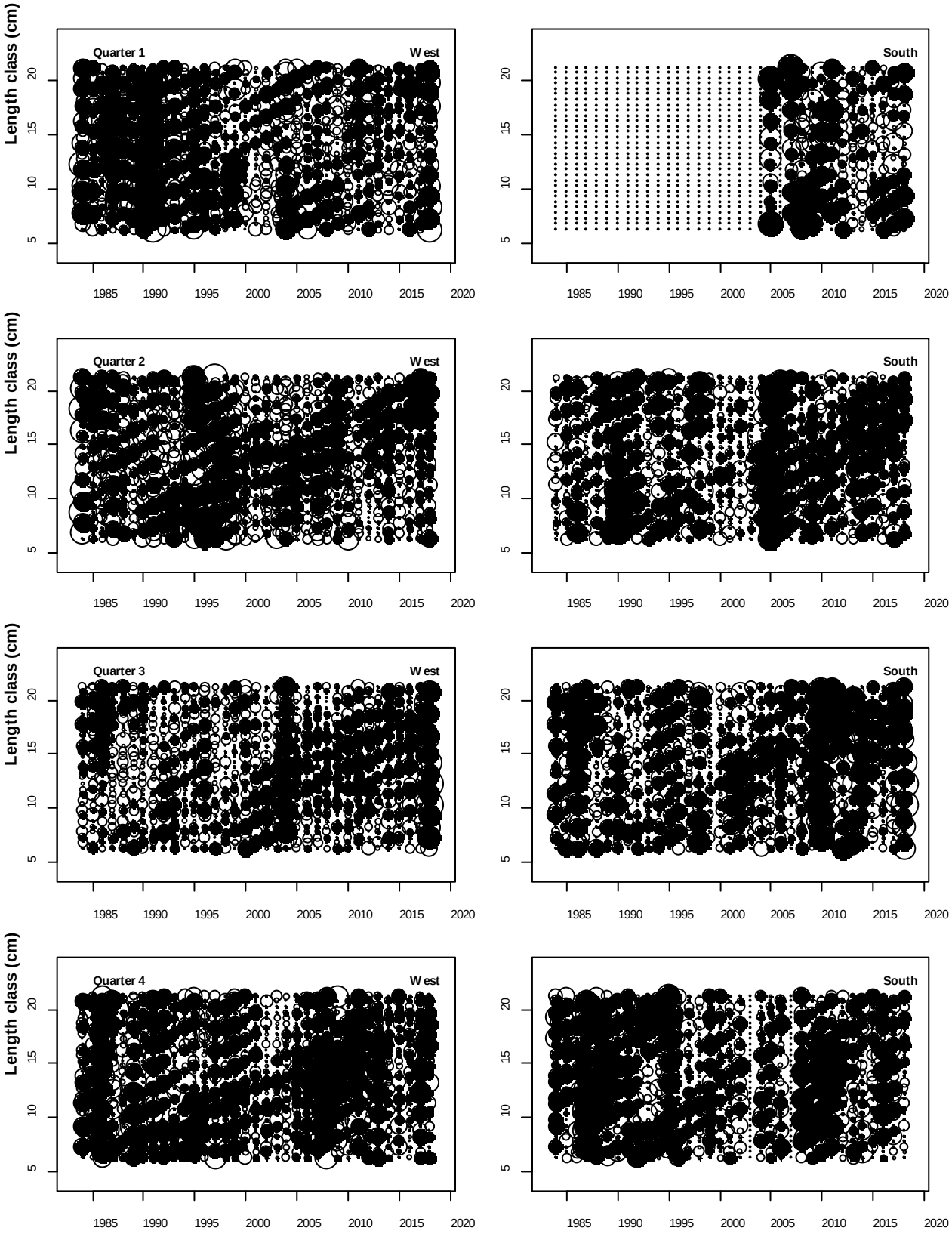

Figure 9. Residuals from the fit of the model predicted proportions-at-length in the quarterly commercial catch to the observed proportions.

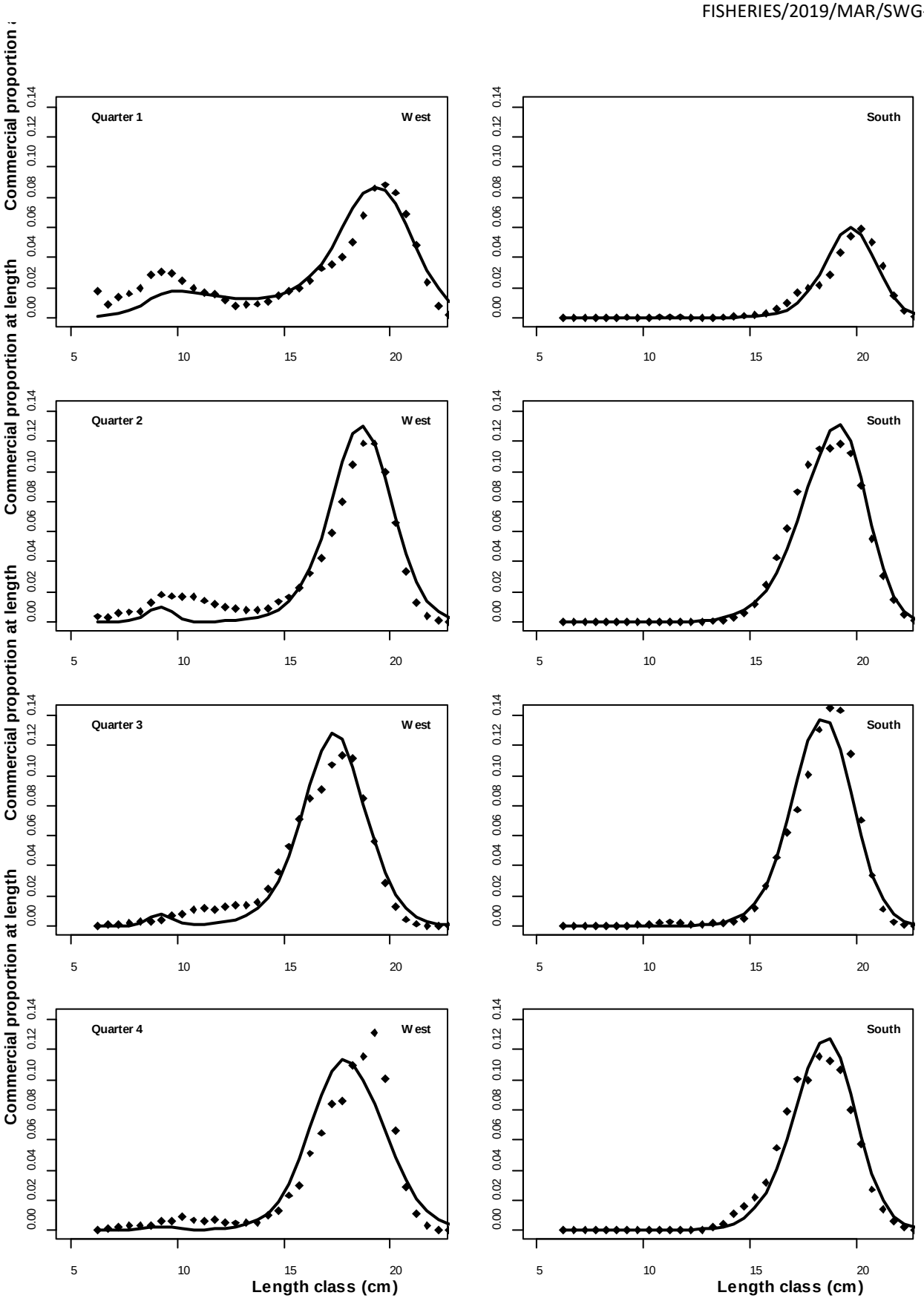

Figure 10. Average (over all quarters and years) model predicted and observed proportion-at-length in the commercial catch (top row), and average (over all years) quarterly model predicted and observed proportions-at-length in the commercial catch (subsequent rows).

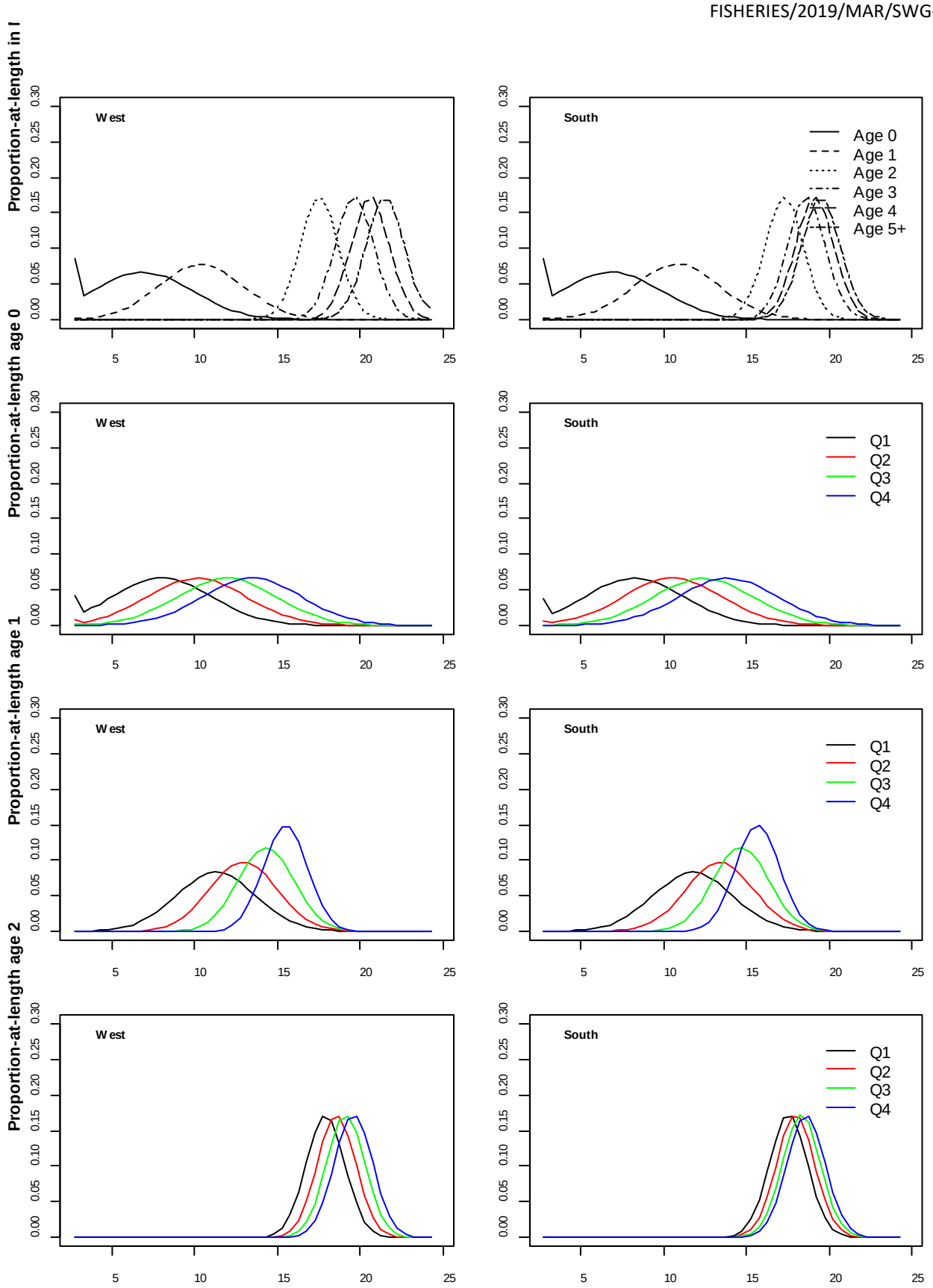

Figure 11. The model estimated distributions of proportions-at-length for each age **in 2010**, given at the time of the biomass survey (1 November, top row), and middle of each quarter of the year (corresponding to the times commercial catch is modelled to be taken) for age 0, 1 and 2 (subsequent rows).

Figure 12. The model estimated proportion of west component sardine infected with the parasite between 2008 and 2018. (Annual infection rate is arbitrarily assumed to be 0 prior to 2008.)

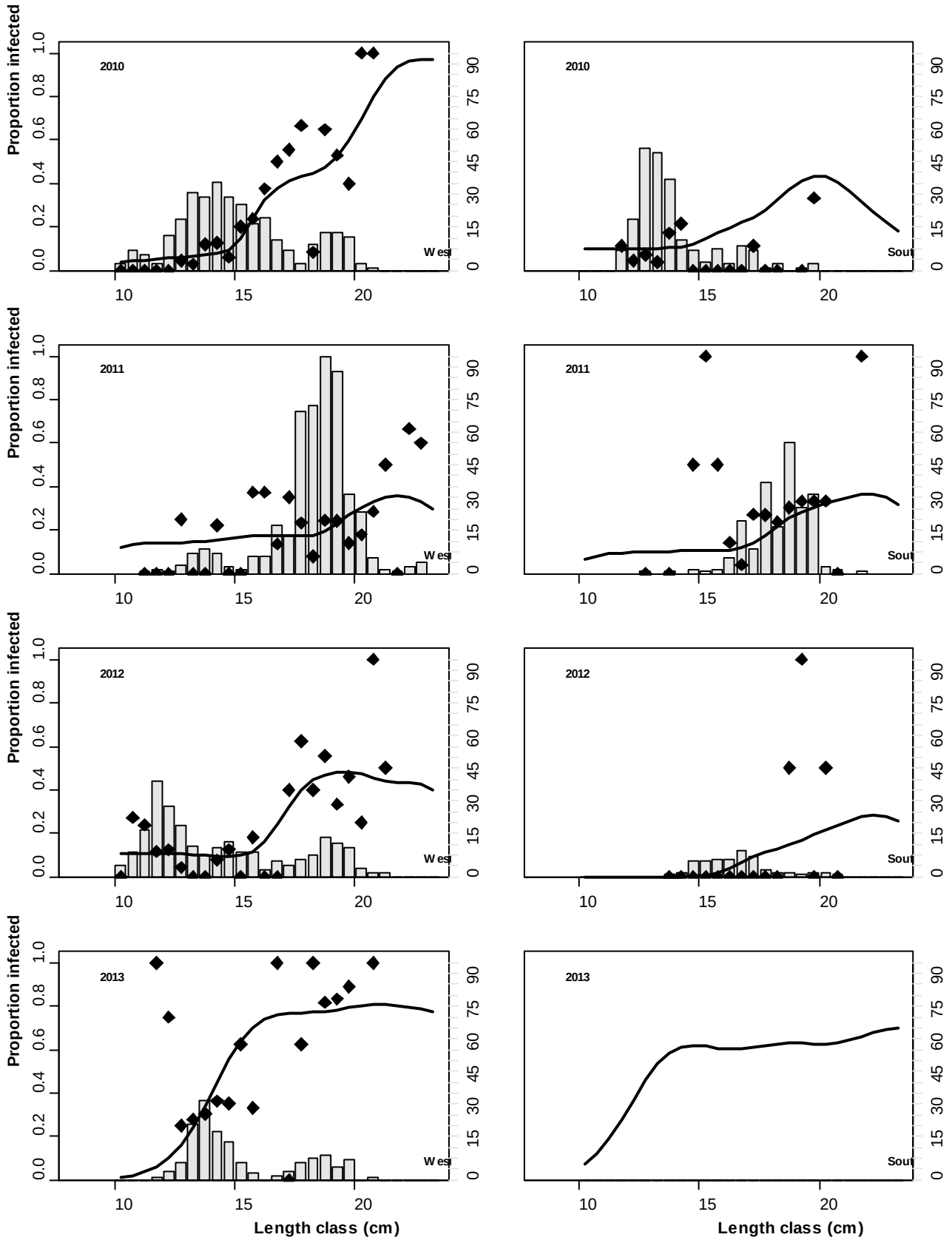

Figure 13. The model estimated proportions-at-length of west and south stock sardine infected with the parasite (i.e. parasite prevalence-by-length) between 2010 and 2018 together with the observed proportions-at-length. The sample size for each length class is given by the grey bars, plotted against the right vertical axis.

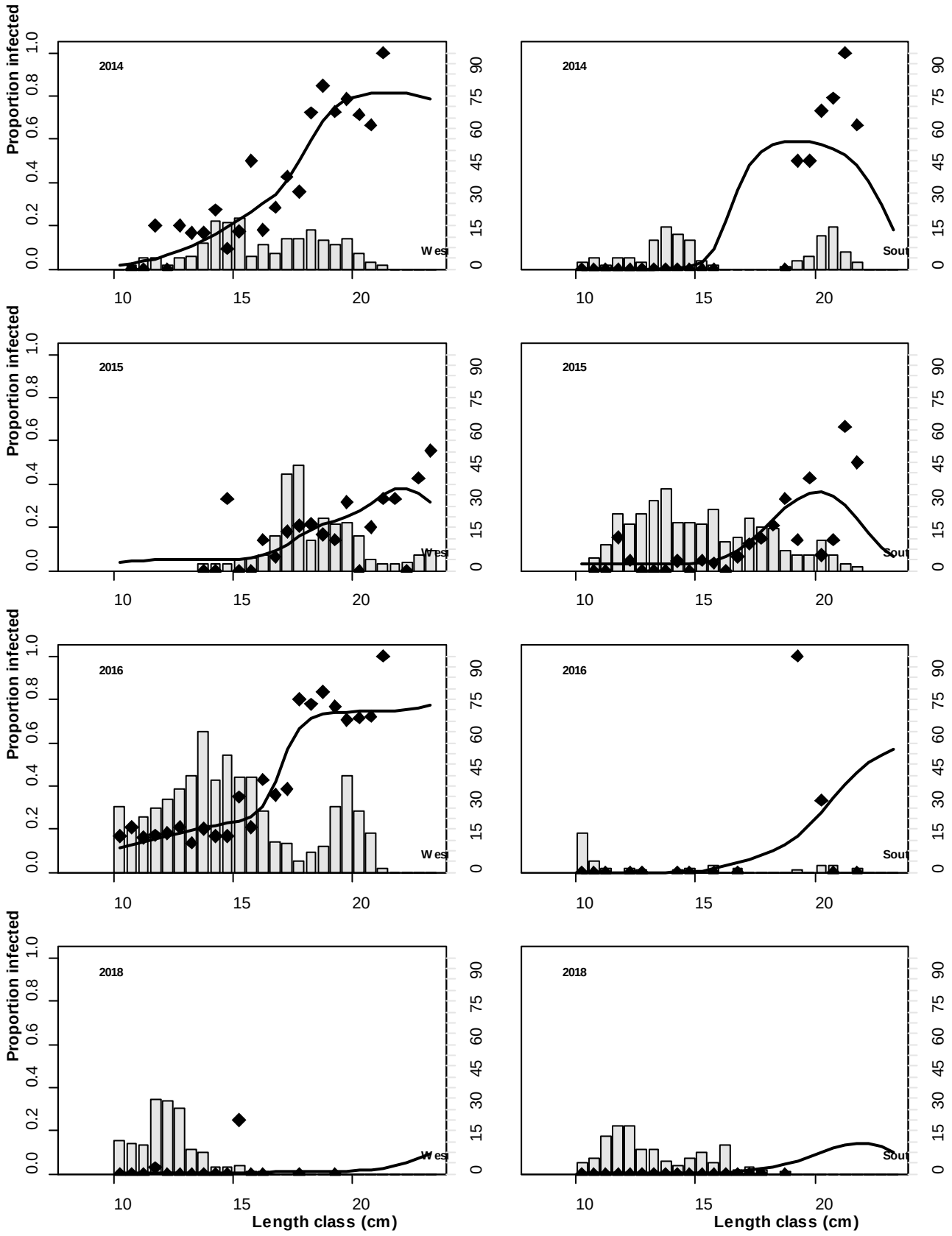

Figure 13 (continued).

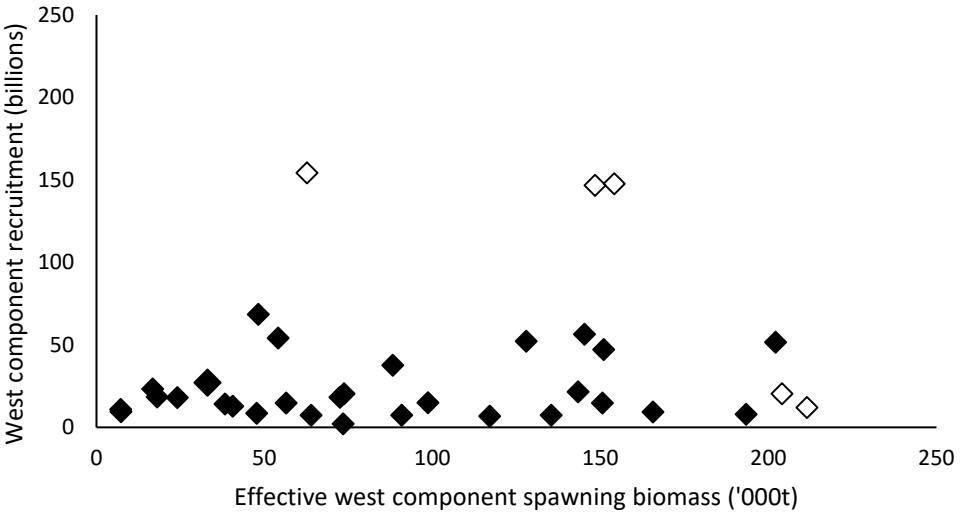

Figure 14. Model predicted sardine recruitment (in November) plotted against effective spawner biomass from November 1984 to November 2017.

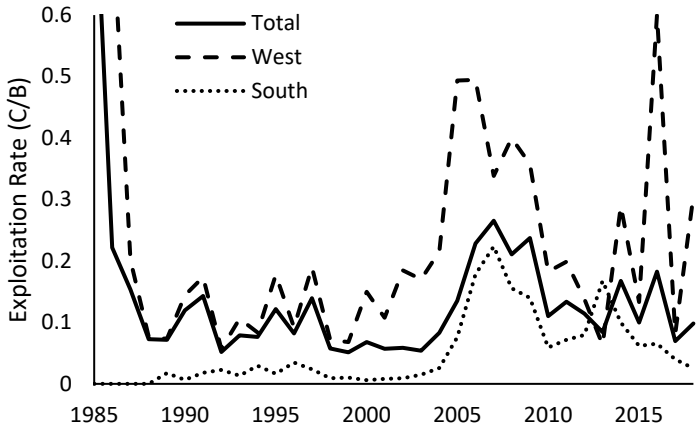

Figure 15. The exploitation rate (simply calculated as the observed annual (Nov-Oct) catch tonnage as a proportion of the model predicted total biomass).

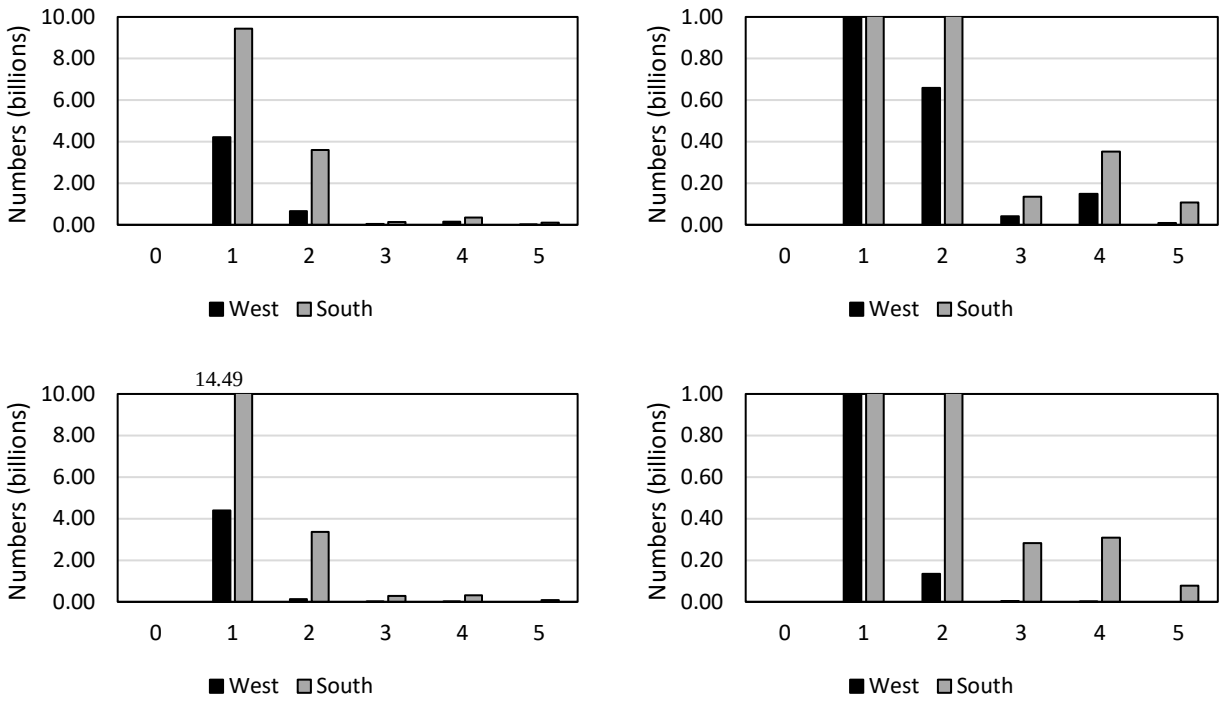

Figure 16. The point estimates of numbers-at-age in 2018 estimated by de Moor (2019) (upper plots) and this revised model (lower plots). The right hand plots are a repeat of the left hand plot, but with a different vertical axis range.